FY12 Line-Supported Bio-Medical Initiative Program: Advanced Photoplethysmography (PPG) Sensors for Operational and Casualty Care Medicine

A.J. Swiston
M. Raj

19 November 2012
Reissued 11 February 2013

Lincoln Laboratory

MASSACHUSETTS INSTITUTE OF TECHNOLOGY

LEXINGTON, MASSACHUSETTS

This technical report has been reviewed and is approved for publication.

FOR THE COMMANDER

Gary Tutungian
Administrative Contracting Officer
Enterprise Acquisition Division

Massachusetts Institute of Technology
Lincoln Laboratory

FY12 Line-Supported Bio-Medical Initiative Program: Advanced Photoplethysmography (PPG) Sensors for Operational and Casualty Care Medicine

A.J. Swiston
Group 48

M. Raj
Group 86

Project Report LSP-40

19 November 2012
Reissued 11 February 2013

Lexington   Massachusetts

This page intentionally left blank.

ABSTRACT

Visible and near-infrared light interact via absorption and scattering with biomolecules, and a number of diagnostic tools based upon these interactions have been developed to indicate pathophysiological states and normal and diseased tissue. Additionally, the cyclic nature of these absorption or scattering events, such as those arising from cardiovascular or pulmonary physiology, has recently been shown to indicate trauma and cardiovascular status. The most commonly encountered diffuse optical technique is pulse oximetry, a form of photoplethysmography (PPG), where the distinct absorption behavior of oxygenation and non-oxygenation hemoglobin molecules forms a basis for determining arterial blood O_2 saturation levels (SpO_2). New analysis algorithms have shown that PPG can be used to indicate a variety of physiological conditions beyond hypoxic hypoxemia (i.e., low SpO_2) including noncompressible hemorrhage, a condition notoriously difficult to diagnose without CT or MRI capabilities, and cardiac output, a variable difficult to measure in real time noninvasively.

With support from the FY12 Biomedical Initiative Line, we embarked on a size, weight, and power (SWaP) analysis of PPG sensors, and collaborated with Professors Ki Chon and Yitzhak Mendelson from Worcester Polytechnic Institute to build a prototype ultra-low SWaP sensor. This report gives background and motivation for why PPG sensing is an important physiological modality, and details on the SWaP analysis and prototype development.

This page intentionally left blank.

ACKNOWLEDGMENTS

This page intentionally left blank.

TABLE OF CONTENTS

This page intentionally left blank.

LIST OF ILLUSTRATIONS
(Continued)

1. INTRODUCTION

Plethysmography is the measurement of the relative size of an organ; *photo*plethysmography (PPG) is measuring this size using light. A particular and ubiquitous application of PPG is in pulse oximetry, whereby the oxygenation saturation of arterial blood is measured. Pulse oximetry requires absorption measurements of oxygenated (HbO_2) and deoxygenated hemoglobin (Hb) at 940 nm (near-IR) and 660 nm (red); Hb and HbO_2 display markedly different absorption behavior around these wavelengths (see Figure 1). Additionally, oximetry requires precise measurement of the peripheral vasculature's cyclically changing volume (and hence the need for plethysmography and not just absorbance measurements; see below) [1]. Since these wavelengths are often unobscured by absorption from other biomolecules (water, most importantly), the relative quantity of Hb to HbO_2 (i.e., SpO_2) may be determined noninvasively. The advent of such a noninvasive arterial oxygen saturation measurement was a significant step forward in clinical medicine, since low SpO_2 values may be used to indicate a host of pathological pulmonary conditions such as COPD, airway obstruction, and edema [2].
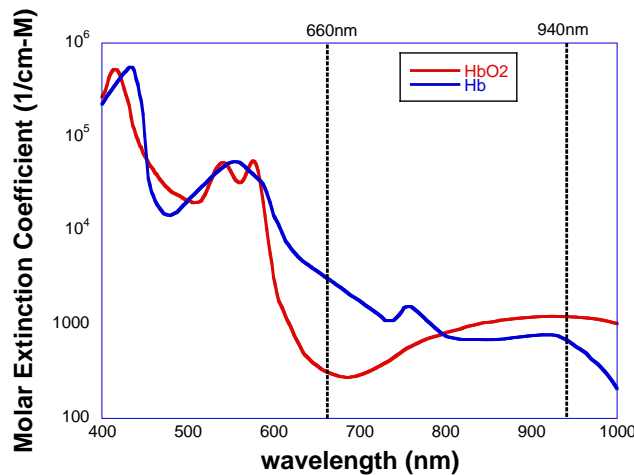
Figure 1: Absorption spectra of oxygenated and deoxygenated hemoglobin. The two most commonly used wavelengths in pulse oximetry, 660 nm and 940 nm, are indicated. Created using data from [3].

The variable of greatest interest from pulse oximetry is the oxygen saturation of *arterial* blood. As mentioned above, oximetry relies upon PPG to measure the cyclic filling (dilation) and emptying (contraction) of the peripheral vasculature; relying on the assumption that only the arteries and arterioles have sufficient pressure to dilate and contract during systole, then only arterial blood will display peristaltic optical absorption behavior [1]. Figure 2 shows a typical PPG waveform, along with several

absorbance contributors. To derive SpO$_2$ values, similar PPG waveforms at the two wavelengths of interest are measured, normalized, divided by one another to give a ratio of intensities, and compared against an empirically-derived look-up table which relates SpO$_2$ and the signal ratios. (The details of this analysis are beyond the scope of this paper, and full details may be found in [1].)
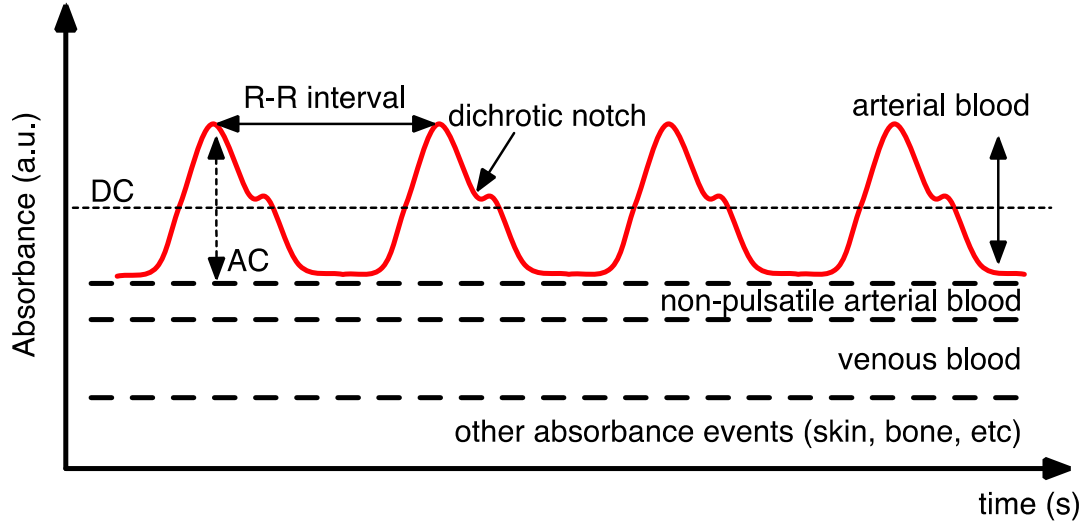
Figure 2: A notional PPG waveform showing the cyclical nature of the signal and several absorbance and scattering contributors. Note that the arterial blood is assumed to be the only contributor to the pulsatile signal, and the difference between the signal's peak and trough is referred to as the high-frequency AC component. The DC component reflects all other absorbance events and is the average value of the AC component. Adapted from [1, 4].

Immediately, additional variables of interest are obvious from the PPG waveform, most notably the heart rate (HR) and the derived variable heart rate variability (HRV). However, the complex pulsatile nature of the PPG waveform is an often underutilized data stream in the technique. PPG gives information on the cyclic and ever-changing state of the peripheral vasculature. A more realistic PPG waveform may be found in Figure 3 [5], where the high-frequency AC component is shown superimposed on the lower-frequency DC component. These multiple frequency bands indicate different aspects of cardiovascular (AC) and respiratory (DC) physiology, and only very recently have the complex rhythmic behavior of the PPG waveform been leveraged.
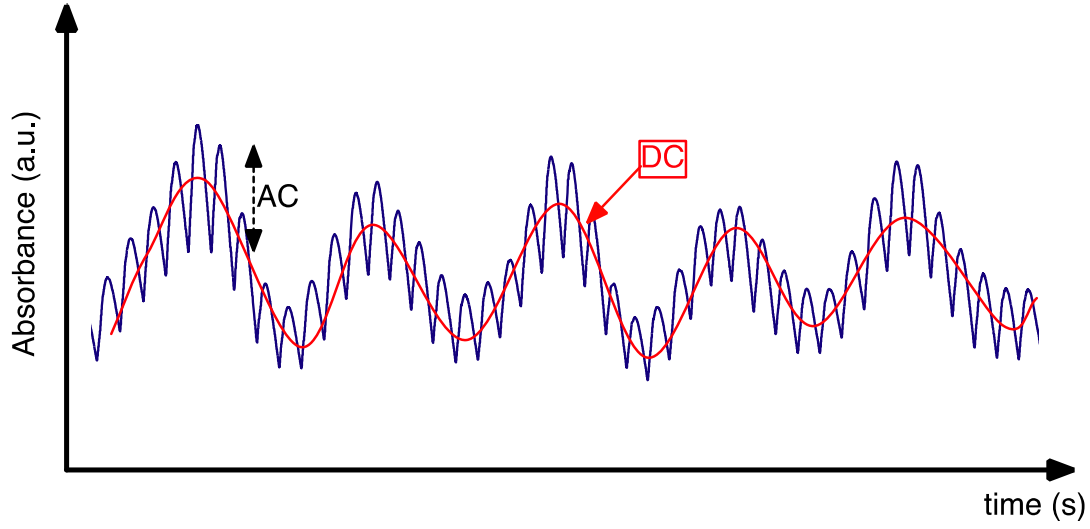
Figure 3: A realistic PPG waveform collected from the earlobe. The high-frequency AC component (variations in blue line) is overlaid on a much lower frequency DC component (variations in red line) that reflects respiratory effects on absorbance. Adapted from [5, 6].

Two notable applications – detection of hemorrhage and cardiac output – will be summarized below. Both of these applications make use of the full rhythmic waveform of the PPG signal, rather than simply using the pulsatile nature to 'gate' data as arterial versus venous absorbance contributions. These two examples are clear indicators of the value of expanding the use of PPG to measure numerous physiological parameters that may either be impossible or inconvenient to access. These applications also emphasize how temporally granular physiology can be – scalar values such as heart rate or blood pressure are hardly comprehensive descriptors of the highly dynamic and transient systems that comprise human physiology.

This page intentionally left blank.

2. CASUALTY CARE MEDICINE: DETECTION OF HEMORRHAGE

Uncontrollable, uncompressible truncal hemorrhage is an extremely common trauma seen on the battlefield, accounting for 83–87% of "potentially survivable deaths" by some estimates [7]. Furthermore, identifying hemorrhage is not possible based on standard vital signs available to the combat medic or trauma physician (systolic/diastolic blood pressure, mean arterial pressure, SpO_2, end-tidal CO_2, heart rate, and respiration rate) [8–10]. For example, Figure 4 below plots standard vital signs against blood volume loss [10].
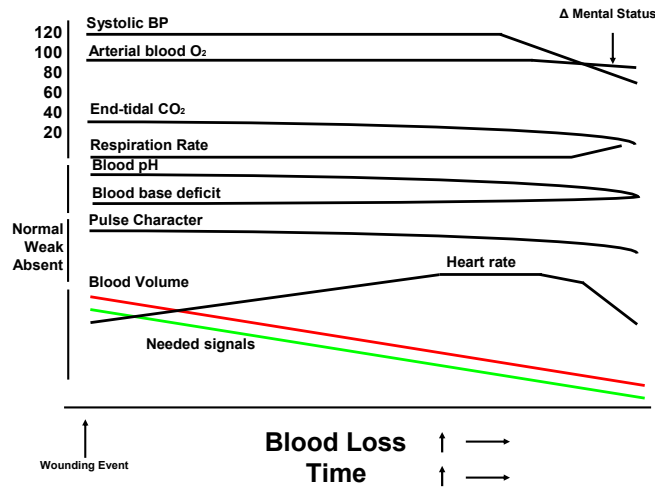
Figure 4: Time course of standard vital signs following a hemorrhage-inducing event. Note that no easily detectable signals are observed until immediately prior to hemodynamic decompensation and unconsciousness. Taken from [10].

The reflexive compensatory response for maintaining mean arterial pressure during hemorrhage (systemic vasoconstriction, locally-controlled constriction in ischemic tissues, increased cardiac contractility, increased heart rate in only some patients [11, 12]) is capable of maintaining clinically normal values [10] for up to 40–50% blood volume loss [9, 10], a fact noted as far back as World War II [13]. Without advanced imaging capabilities such as CT or MRI (which is often precluded because of embedded shrapnel), the medic or trauma physician has little information to support the decision to begin fluid resuscitation [14]. Considering that preventing cerebral hypoperfusion is of utmost importance (cerebral tissue hypoxia onsets in around 60 s [1]), a better indication of internal hemorrhage is desperately needed to address and treat what may otherwise be preventable deaths.

2.1 RECENT ADVANCES IN PPG ANALYSIS FOR HEMORRHAGE DETECTION

Using a technique known as lower body negative pressure (LBNP), researchers are able to experimentally mimic central volume loss in a controllable, reversible, and medically ethical manner. Negative pressures are applied to the lower body (below the iliac crest), leading to shunting of blood away from the thorax and head. Convertino et al has shown that this procedure is physiologically similar to traumatic hemorrhage; it too reduces tissue oxygen perfusion, tissue pH, and eventually leads to severe hypotension and hemodynamic decompensation (see references 10 and 15, and references therein).

Recently, advanced machine learning algorithms have been developed [10, 16], which are capable of not only detecting hemodynamic compensation during hemorrhage, but of predicting when an individual will begin decompensating. These algorithms are based upon identifying features in the PPG waveform, such as the area under the curve, pulse amplitude, or pulse width at half-maximum [17], then finding cross-correlates in time. Such algorithms require to be trained on a 'truth' dataset, which LBNP experiments can provide as a function of pressure applied and onset of decompensation. Using this approach, Convertino et al. trained their algorithm on 27 volunteers, and tested on the 28th. The results of this test are shown in Figure 5.
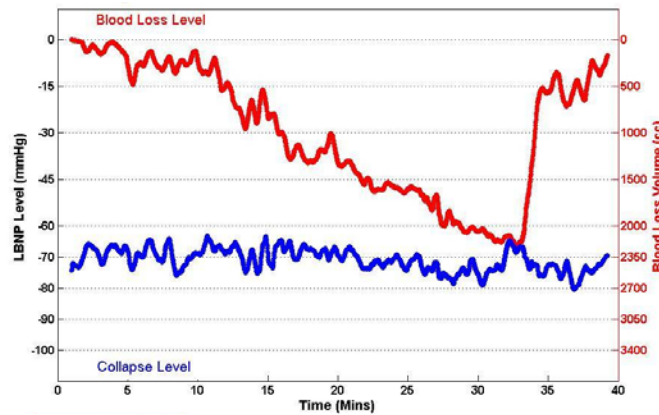
Figure 5: The machine learning algorithm is capable of both predicting the point at which hemodynamic decompensation will occur (blue line) and the instantaneous blood loss level as projected from LBNP pressure (red line). When the blue and red lines meet, decompensation occurs and the LBNP experiment is ended. From [10].

2.2 CONCLUSIONS ON HEMORRHAGE DETECTION

This ability to predict and quantify hemorrhage levels is a major innovation for field triage and combat casualty care. Continued investigation is required for implementing these algorithms in operational contexts which suffer from additional complications (namely, motion artifacts, as PPG is

particularly susceptible to movement of both the patient and the detector [18]) not found in a laboratory research setting. These types of real trauma tests are currently being conducted by the US Army Institute for Surgical Research in helicopter-based medical evacuations in the San Antonio, Texas, area [19].

This page intentionally left blank.

3. OPERATIONAL MEDICINE: CARDIAC OUTPUT

Cardiac output (CO) is an essential indicator of cardiovascular health, and diseases of the cardiovascular system are often comorbid with changes in CO [20]. Knowledge of an individual's cardiac output during combat or training operations would be indicative of pathological conditions, such as heat exhaustion, changes in total peripheral resistance (vasoconstriction/dilation), cardiogenic shock, and changes in stroke volume. Currently, CO measurement is measured invasively, which isn't possible in operational contexts nor is amenable to real-time, remote measurement.

One exciting future research avenue would investigate the use of noninvasive PPG sensing to measure CO. Recent work has shown how venous blood saturation levels may be measured via PPG [4]. As mentioned above, the DC component of the PPG signal is indicative of changes in respiratory status. More recent understanding on the nature of venous compartment pulsatility [21] has revised the belief that veins do not contribute to the cyclic absorbance of the PPG signal. For instance, mechanical ventilation is thought to affect the venous compartment volume by increasing pressure on the vena cavae during inspiration [22]. Such behavior can be understood analogously to the coupling of the Bainbridge reflex with respiratory sinus arrhythmia (RSA); heart rate increases during inspiration (RSA), since compression of the vena cavae momentarily increases venous pressure and thus, heart rate via the Bainbridge reflex. While the presence of the Bainbridge reflex in humans is still contested [23], the frequently observed RSA phenomenon indicates that subtle changes during the respiratory cycle may indeed affect vasculature distal to the thorax and capable of measurement via PPG.

Recent work by Walton et al. [4] has indicated that modulation of the DC component will give *venous* saturation, whereas modulation in the AC component gives *arterial* saturation (as is done in PPG-based oximetry). These two distinctions are shown in Figure 6.

$$R = \frac{(|AC|/DC)_{Red}}{(|AC|/DC)_{IR}} \qquad R = \frac{(|DC|/DC)_{Red}}{(|DC|/DC)_{IR}}$$
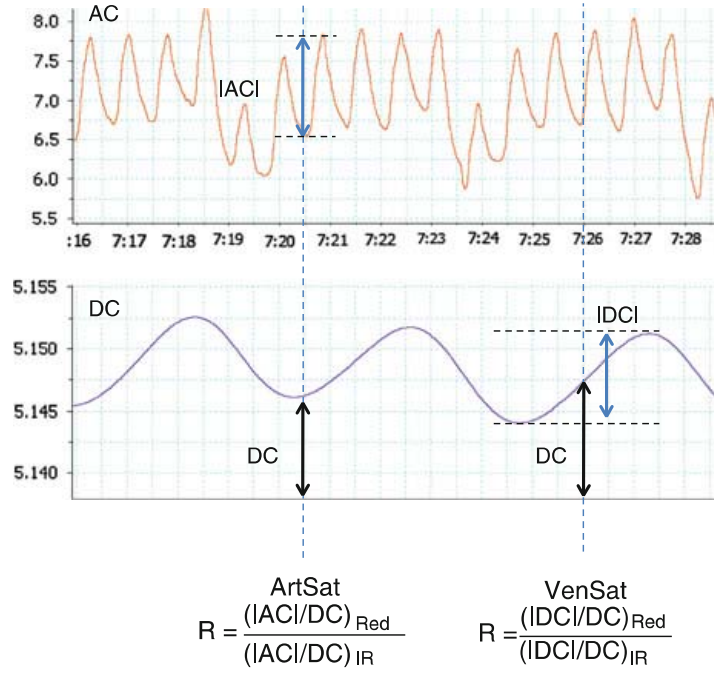
Figure 6: Real PPG waveforms with AC vs. DC components designated. The rise in the AC component is due to increased arterial saturation during systole. A rise in the DC component is due to increased absorbance during inspiration (and decrease in venous compartment volume due to pressure on the vena cava), which is directly related to the frequency of mechanical ventilation. From [4].

These analysis algorithms need to be verified clinically by comparing the computational result with venous blood gas measurements, but the ~85% values reported are what would be physiologically expected [4]. If these methods are verified to be accurate, this would enable a noninvasive arteriovenous oxygen difference measurement; such information could then be used in the Fick equation (explained below) to give an approximate value for cardiac output.

3.1   THE FICK PRINCIPLE AND CARDIAC OUTPUT

The Fick Principle relates the volume of oxygen consumed by an organ to the blood flux through that organ. If instead of an organ, the body as a whole is considered, and assuming a closed system with no accumulation (i.e., no blood loss nor oxygen collection without consumption), a mass-balance equation may be written as follows:

$$VO_2 = (CO \times C_{a,O_2}) - (CO \times C_{v,O_2}) \tag{1}$$

10

where VO_2 is the volume of oxygen consumed by that organ per minute (mL/min), CO is the cardiac output (in mL blood/min) and $C_{a,O2}$ and $C_{v,O2}$ are the concentrations of oxygen (mL O_2/100 mL blood) in the afferent artery (arteriole) and efferent vein (venule), respectively. The behavior of this equation may be seen in Figure 7, which shows cardiac output as a function of $C_{v,O2}$, assuming $C_{a,O2} = 20$ mL O_2/100 mL blood.
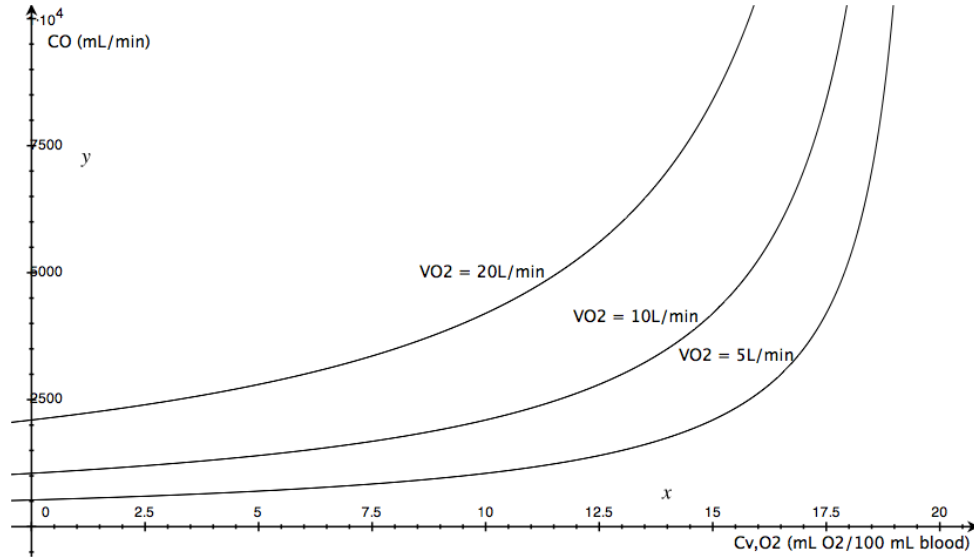
Figure 7: Cardiac output (CO) as a function of $C_{v,O2}$, and thus the arteriovenous oxygen concentration difference. Each contour assumes a constant value of VO$_2$, and PO$_2$/P$_{atm}$ = 0.21.

Figure 7 shows the expected behavior for an aerobically metabolizing system: as the concentration of VO_2 is constant along a contour, low arteriovenous oxygen differences (i.e., high $C_{v,O2}$) require a larger flux (i.e., CO) of blood to deliver the inspired VO_2. Conversely, high arteriovenous oxygen concentration differences (low $C_{v,O2}$) require lower blood flux to deliver inspired VO_2, as larger quantities of O_2 are unloaded per unit of blood.

Equation (1) can be rearranged and expressed in terms of tidal volume *TV* (mL) and *RR*, the minute respiratory rate (breaths/min):

$$CO = \frac{VO_2}{C_{a,O_2} - C_{v,O_2}} \cong \left(TV \times \frac{P_{O_2}}{P_{atm}} \right) \frac{RR}{C_{a,O_2} - C_{v,O_2}} \tag{2}$$

11

where P_{O2} is the partial pressure of oxygen, P_{atm} is the atmospheric pressure (we will not assume a particular value for P_{atm}, since operations may occur at significant elevations where $P_{atm} < 1$ atm). Equation (2) contains all variables that may be measured noninvasively, and if a value for *TV* is assumed based on activity level (or approximate metabolic rate) and an individual's $VO_{2,max}$, then spirometry equipment isn't required. Using the proposed method above, a PPG sensor could measure $C_{a,O2}$ and $C_{v,O2}$, as well as *RR* by measuring the peak-to-peak distance of the waveform's DC component (see Figure 6) [24].

3.2   CONCLUSIONS ON CARDIAC OUTPUT MONITORING

The recent work on venous saturation levels open exciting opportunities in noninvasive cardiac output monitoring. Despite the importance of CO in indicating cardiovascular health and disease state, such measurements are not done routinely. With appropriate correlative studies to establish the precise relationship between DC component modulation and venous saturation (as had been done with AC component modulation and arterial saturation), PPG sensors may provide a noninvasive, and perhaps ambulatory, CO monitor for both operational and casualty care medicine. We feel this to be an exciting area of research worth pursuing immediately for its combination of sensor simplicity (a conventional PPG) and existing acceptance within the clinical community.

4. MIT LL PROTOTYPE HARDWARE DESIGN

Optimizing a PPG sensor for size, weight, and power (SWaP), requires an extensive system analysis that evaluates each individual components' size and energy contribution. The architecture is broken up into three main components: the sensor transducer, which uses optical energy modulated by blood flow; the analog front end (AFE), which amplifies and filters the received signal; and the digital backend (DBE), which digitizes the analog data and stores it into local memory for long term storage or wireless communication. Each of these subsystems affects the overall longevity of the device and its form factor, driving a set of concepts of operation (CONOPS) that the PPG sensor can be used in. For the purpose of this analysis, the sensor was designed to operate under the following CONOPS:

1. 72 hours of continuous operation

2. Sensor placement in an inconspicuous location (e.g., forehead, sternum)

3. Wirelessly transmit data locally stored on sensor

To achieve these mission goals, an analysis of the system architecture is necessary. PPG sensor systems do not vary too much in terms of architecture or type of components. The specific component attributes (i.e., power consumption, device footprint, and weight) separate the power hungry, heavy units from the energy efficient, light and mobile ones. The relevant hardware blocks of the MIT LL sensor can be seen in Figure 8, divided into the appropriate category.
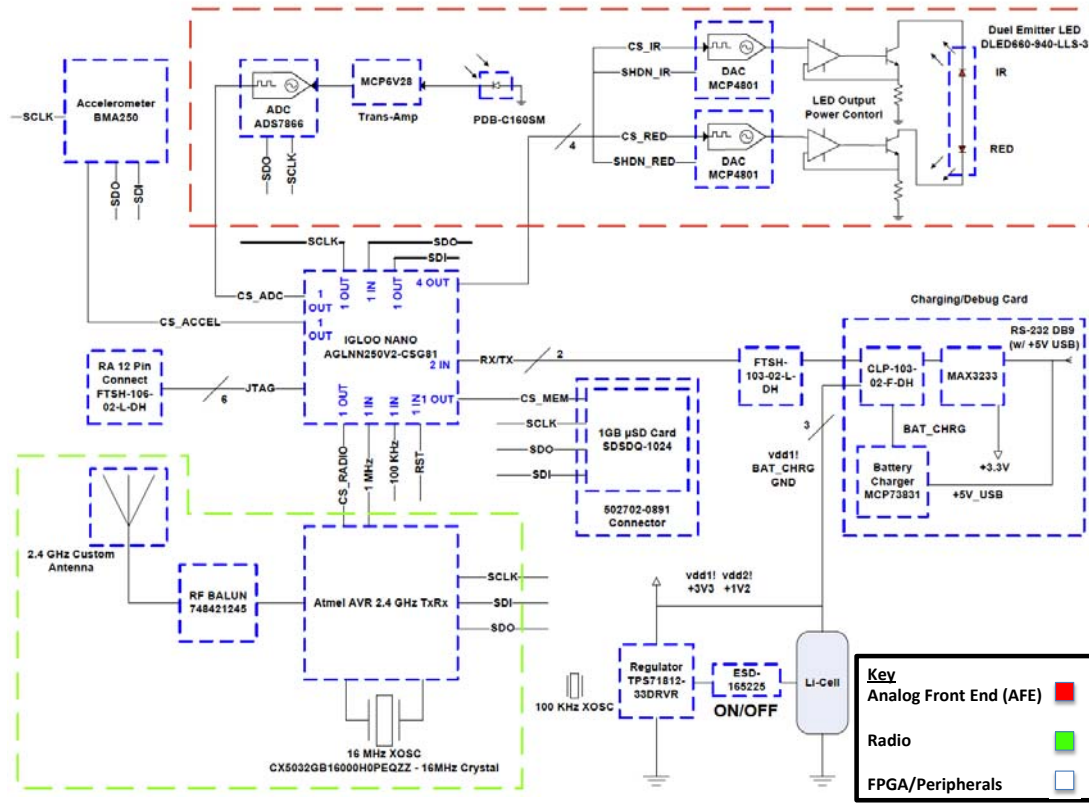
Figure 8: PPG sensor system architecture.

The AFE is composed of a the following: 1) dual-emitter LED package, containing both red (660 nm) and near IR (940 nm) wavelengths; 2) red/NIR enhanced photodiodes to transduce optical energy into electrical energy; 3) transimpedance amplifier (TIA) to amplify and filter the input signal; and 4) analog-to-digital converter (ADC) to digitize the analog information.

The radio includes a readily available solution from Atmel: a 2.4 GHz radio with 802.15.4 (Body-Area Network) and Zigbee compatible communication protocols. A custom-designed antenna, fabricated on the final printed circuit board, serves to complete the wireless link with the necessary peripheral components (e.g., RF balun, 16 MHz crystal). The intent of a wireless radio is to allow the PPG sensor to communicate with an external hub that a warfighter could wear for all Personal-Area Network (PAN) sensors.

The salient pieces of the digital core include the field programmable gate array (FPGA), flash memory, and digital, tri-axis accelerometer. Running on a Serial Peripheral Interface (SPI) bus, the FPGA controls and consolidates information to and from all the peripheral devices on the PPG sensor.

Given the option of a fully customized, Application Specific Integrated Circuit (ASIC) solution or one made up of commercial-off-the-shelf (COTS) components, metrics such as time and resources need to be considered; this led to a choice of using COTS components. In addition, our analysis showed that two components that were most constrained by both power and size are the LEDs and battery, respectively. These two parts of the system are not readily optimized in an IC design process, making the choice of a COTS implementation all the more easy.

4.1   SIZE, WEIGHT, AND POWER ANALYSIS

The final PPG sensor was designed using COTS components (see Appendix A). An energy budget model, programmed in Matlab, was developed to allow a user to quickly adjust design parameters, type of COTS, and CONOPS definitions for the sensor. The resulting output of the model was the expected longevity of the sensor given these various parameters. Figure 9 shows the energy budget of the PPG sensor running off a 3.0 V, 110 mA-Hr battery.
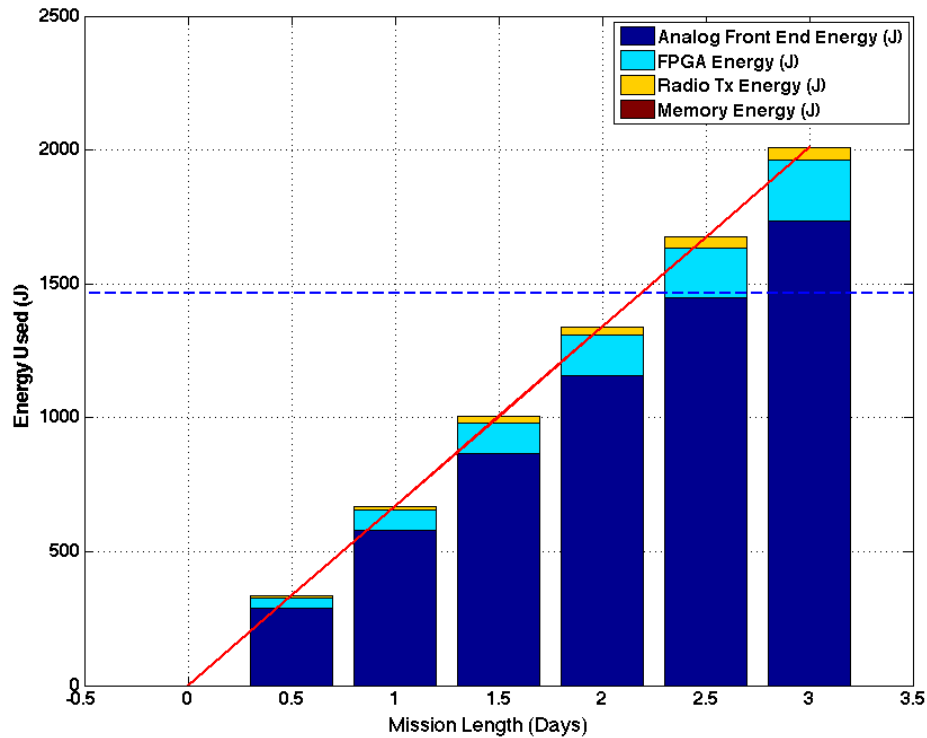

Figure 9: PPG sensor energy distribution versus mission length.

15

For the purposes of this design, the components were readily available from online vendors and distributors (See Appendix A – Bill of Materials). As mentioned previously, the two components that imposed the most constraints on the design are the LEDs and battery. Figures 10 and 11 show the breakdown of power and size for the AFE and sensor, respectively. As can be seen from the graph, the LED dominates the power profile of the AFE, with the photodetector circuit requiring the next highest amount of energy. This implies that if either the LED output power is minimized or the photodetector circuit is optimized for low-light levels, the AFE power use can be greatly reduced, extending the longevity of the device. This can be implemented by duty-cycling the LED output [1]. That is, for 50% duty-cycle at a given sampling period, say 10 msec, the LED will be on 5 msec. By adjusting this duty-cycle value, one can drastically reduce the amount of time the LED is on and, ultimately, the amount of energy it uses. However, this variability is limited by the sensitivity of the photodetection circuit and how effectively it can sense the PPG signal in low-light conditions. Fortunately, modern photodetector and amplifier designs have very good sensitivity, to the point where the LED power can be backed off considerably [25].

AFE Energy Used vs. Mission Length

PPG Sensor Volume by Components
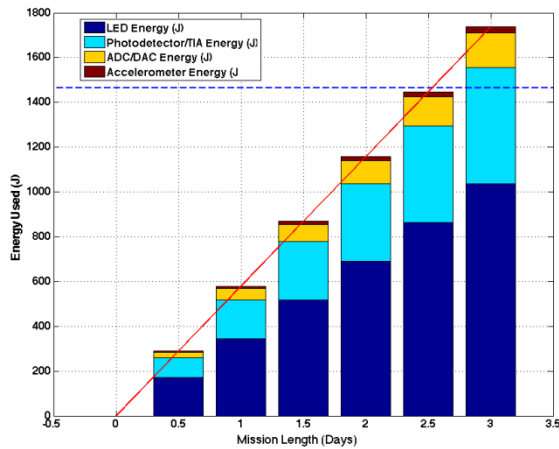
Figure 10: Analog front-end energy distribution versus mission length, which shows battery lifetimes of over 48 h for a 110 mA-hr battery.
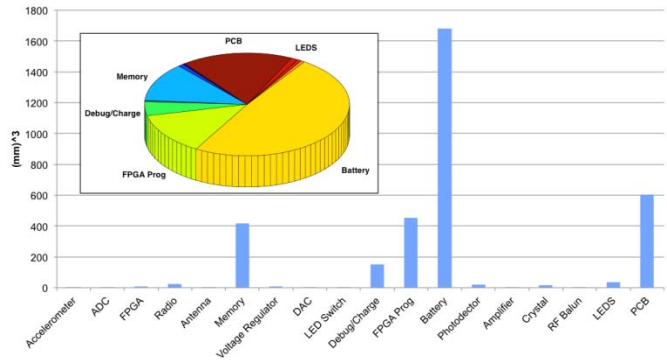
Figure 11: PPG sensor component volume breakdown.

4.2 MIT LL PROTOTYPE HARDWARE DESIGN

Based on this analysis and the implications of Figure 11, COTS components were chosen to mitigate both power and size restrictions. Figures 12 and 13 show the resulting PPG sensor, front and back, and the overall size. This fully integrated system has an antenna, micro-SD memory card holder, 2.4 GHz radio, FPGA, tri-axial accelerometer, and LED/photodetectors for sensing the PPG waveform.

PPG Sensor (Front)	PPG Sensor (Back)
Figure 12: Air-facing side of PPG sensor. Salient components include micro-SD card, power regulators, and custom PCB antenna.	*Figure 13: Skin-facing side of PPG sensor. Salient components include LEDs, photodiodes, FPGA, and radio.*
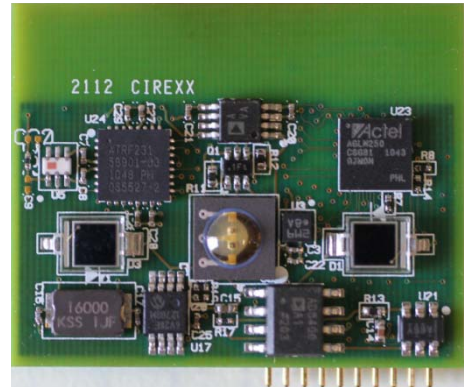
The custom antenna was designed to be centered about 2.45 GHz with approximately 100 MHz of bandwidth. This resulted in the radiation pattern seen in Figure 15. It is clear from this picture that the sensor will be able to transmit and receive data in almost any direction, enabling communication with some sort of PAN communications hub or other device.

PPG PCB Antenna Design	PPG Antenna Radiation Pattern
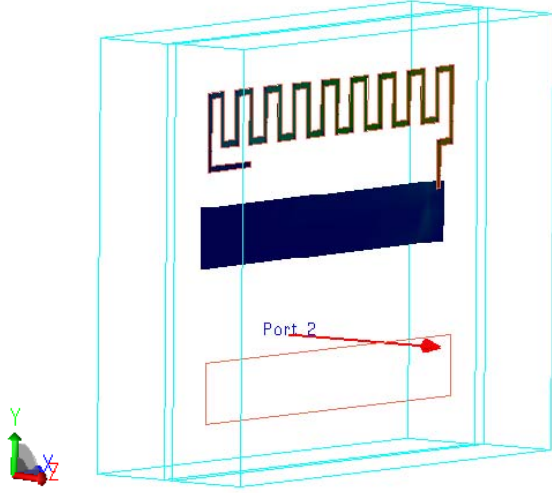
Figure 14: 3-D representation of custom antenna on PPG sensor board.
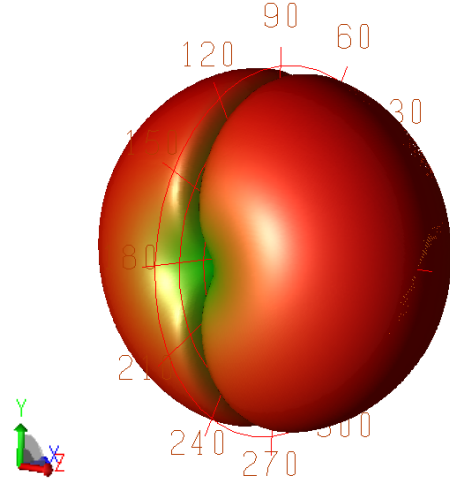
Figure 15: Antenna radiation pattern.

4.3   PRELIMINARY DATA

The complete hardware and software design and implementation were done over the span of four months. In that time, several tests were conducted to determine the sensor's ability to detect a person's PPG waveform. Figure 16 shows the results from one such test; Figure 16(a) corresponds to the data seen on an oscilloscope at the output of the AFE, before digitization in the DBE. While the waveforms appear clean and clearly show peaks that are congruent with heartbeats, the test was done in a very controlled fashion. That is, the tester was not ambling and had a firm, physical connection with the sensor's front end with a finger over the LED/photodetectors. In a typical scenario, a walking patient will cause motion artifacts to propagate through to the sensor's output, interfering with proper recording [18]. It is unclear whether the onboard accelerometer can mitigate this by actively subtracting motion measurements from the PPG recording, but it is an area of active research and could help enable an ambulatory version of a fully integrated, PPG sensor, such as has been reported [26].
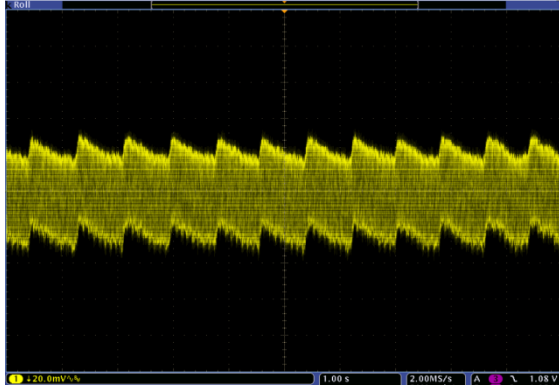
PPG Raw Data	PPG Data Processed in Matlab
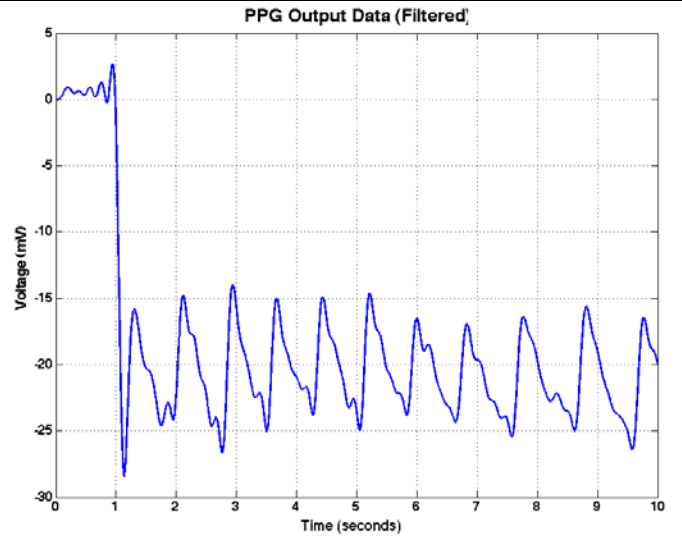
(a)   (b)

Figure 16: PPG trace (a) on an oscilloscope, and (b) after applying a 5 Hz lowpass filter in Matlab.

This page intentionally left blank.

5. CONCLUSIONS AND SUMMARY

Advances in noninvasive medical monitoring have led to expanded use of PPG to new indications. While pulse oximetry has relied on PPG for over 20 years, new processing algorithms and corresponding physiological understanding have recently enabled PPG to sense two conditions notoriously difficult to measure easily and noninvasively, namely, hemorrhage and cardiac output. Internal hemorrhage is one of the leading causes of battlefield mortality, partially due to the inability to quickly diagnose and triage those with the most compromised central volume status. PPG algorithms have been developed that are able to not only measure the level of blood loss, but also individually predict at what point a patient will begin to hemodynamically decompensate. Second, recent work suggests that pulse oximetry need not be limited to measuring arterial saturation, but may be used for venous saturation as well. If these preliminary findings are clinically verified, then noninvasive cardiac output measurements may be possible and perhaps even real time. Expanding the use of PPG to include these two conditions represents new opportunities in combat casualty care, such as enabling remote triage of internal hemorrhage, and operational medicine, where knowledge of CO in real time could be used to alert commanders of team members in physiologically compromised states.

Our SWaP analysis and prototype development points to the possibility of including PPG in the physiological monitoring suite currently under consideration by the Army, as the indication set made possible by real-time PPG data seems to be expanding quickly for conditions of great concern to the U.S. military.

This page intentionally left blank.

APPENDIX A
MIT LL PPG SENSOR BILL OF MATERIALS

Item	Qnty	Partnum	Vendor Partnum	Description
1	1	828-1023-1-ND	BMA250	3-Axis Accelerometer Digital I/F
2	1	296-18216-1-ND	ADS7866IDBVT	IC ADC 12BIT 200KSPS SOT23-6
3	1	1100-1123-ND	AGLN250V2-CSG81	250k Gate 6.1kcell 67 I/O Igloo Nano FPGA
4	1	AT86RF231-ZU-ND	AT86RF231-ZU	AVR MCU 2.4GHz Transceiver
5	1	WM19092CT-ND	502702-0891	Micro SD Card R/A Push-Push Connector
6	1	296-2200901-ND	TPS71812-33DRVR	LDO 1.2, 3.3V
7	1	FTSH-110-02-L-DH	FTSH-110-02-L-DH	20 POS, 2 ROW, Male Header
8	2	PDB-C160SM-ND	PDB-C160SM	Photodetector
9	1	MCP6V28-E/MS-ND	MCP6V28-E/MS	Transimpedence Amp
10	1	478-4362-1-ND	CX5032GB16000H0PESZZ	16 MHz Crystal Oscillator
11	1	732-2230-1-ND	748421245	RF Balun
12	1	568-1635-1-ND	BC847BS,115	TRANS NPN GP 100MA 45V SOT363
13	1	AD8542ARMZ-REELCT-ND	AD8542ARMZ-REEL	IC OPAMP GP R-R CMOS 1MHZ 8MSOP
14	1	DLED-660/940-LLS-3	DLED-660/940-LLS-3	Duel Emitter LED IR/RED
15	2	MCP4801-E/MC-ND	MCP4801-E/MC	DAC 8BIT SGL SPI/VREF 8DFN
16	1	AD8400ARZ1-ND	AD8400ARZ1	IC DGTL POT 8BIT 1K 1CH 8-SOIC
17	2			Generic 0402 10 Ohm Resistor
18	1			Generic 0402 5.1 kOhm Resistor
19	1			Generic 0201 30 Ohm Resistor
20	1			Generic 0201 9.1 kOhm Resistor
21	1			Generic 0805 10 MOhm Resistor
22	4			Generic 0201 1 kOhm Resistor
23	1			Generic 0402 0.1 µF Capacitor

Item	Qnty	Partnum	Vendor Partnum	Description
24	1			Generic 0402 500 nF Capacitor
25	2			Generic 0201 12 pF Capacitor
26	2			Tantalum 0603 10 µF Capacitor
27	4			Generic 0201 1 µF Capacitor
28	7			Generic 0201 0.1 µF Capacitor
29	3			Generic 0402 1 µF Capacitor
30	2			Generic 0201 22 pF Capacitor
31	1			Generic 0201 0 Ohm Resistor

REFERENCES

1.   Webster, J.G., *Design of Pulse Oximeters* 1997, New York, NY: Taylor & Francis Group.

2.   Des Jardins, T.R., *Clinical Manifestations of Respiratory Disease* 1990, Chicago IL: Year Book Medical.

3.   Takatani, S. and M.D. Graham, "Theoretical analysis of diffuse reflectance from a two-layer model." *IEEE Trans. Biomed. Eng.*, 1987. **26**: p. 656–664.

4.   Walton, Z.D., et al., "Measuring venous oxygenation using the photoplethysmograph waveform." *Journal of Clinical Monitoring and Computing*, 2010. **24**(4): p. 295–303.

5.   Allen, J.M., et al., "Photoplethysmography assessments in cardiovascular disease." *Measurement and Control*, 2006. **39**(3): p. 80–83.

6.   Allen, J., "Photoplethysmography and its application in clinical physiological measurement." *Physiological Measurement*, 2007. **28**(3): p. R1–39.

7.   Kelly, J.F., et al., "Injury severity and causes of death from Operation Iraqi Freedom and Operation Enduring Freedom: 2003-2004 versus 2006." *The Journal of Trauma*, 2008. **64**(2 Suppl): p. S21–6; discussion S26-7.

8.   Convertino, V.A., et al., "Physiological and medical monitoring for en route care of combat casualties." *The Journal of Trauma*, 2008. **64**(4 Suppl): p. S342–53.

9.   Dutton, R.P., "Current concepts in hemorrhagic shock." *Anesthesiology Clinics*, 2007. **25**(1): p. 23–34, viii.

10.   Convertino, V.A., et al., "Use of advanced machine-learning techniques for noninvasive monitoring of hemorrhage." *The Journal of Trauma*, 2011. **71**(1 Suppl): p. S25-32.

11.   Brasel, K.J., et al., Heart rate: is it truly a vital sign?" *The Journal of Trauma*, 2007. **62**(4): p. 812–7.

12.   Convertino, V.A., C.A. Rickards, and K.L. Ryan, "Autonomic mechanisms associated with heart rate and vasoconstrictor reserves." *Clinical autonomic research: official journal of the Clinical Autonomic Research Society*, 2011.

13.   Shenkin, H.A., et al., "On the diagnosis of hemorrhage in man; A study of volunteers bled large amounts." *Am J Med Sci* 1944. **209**: p. 421–436.

14.   Blackbourne, L., "1831." *The US Army Medical Department Journal*, 2011. April–June 2011.

15. Cooke, W.H., K.L. Ryan, and V.A. Convertino, "Lower body negative pressure as a model to study progression to acute hemorrhagic shock in humans." *Journal of Applied Physiology*, 2004. **96**(4): p. 1249–61.

16. Henry, I., et al., "Body-Worn, Non-Invasive Sensor for Monitoring Stroke Volume, Cardiac Output and Cardiovascular Reserve," in *Wireless Health* 2011, ACM: San Diego, CA.

17. McGrath, S.P., et al., "Pulse Oximeter Plethysmographic Waveform Changes in Awake, Spontaneously Breathing, Hypovolemic Volunteers." *Anesthesia & Analgesia*, 2011. **112**(2): p. 368–374.

18. Comtois, G., Y. Mendelson, and P. Ramuka, "A comparative evaluation of adaptive noise cancellation algorithms for minimizing motion artifacts in a forehead-mounted wearable pulse oximeter." Conference proceedings: ... *Annual International Conference of the IEEE Engineering in Medicine and Biology Society. IEEE Engineering in Medicine and Biology Society. Conference*, 2007. **2007**: p. 1528–31.

19. Convertino, V.A., 2012: Personal Communication. San Antonio, Texas.

20. Grollman, A., *The cardiac output of man in health and disease* 1932: C. C. Thomas.

21. Wardhan, R. and K. Shelley, "Peripheral venous pressure waveform." *Current Opinion in Anaesthesiology*, 2009. **22**(6): p. 814–21.

22. Natalini, G., et al., "Variations in arterial blood pressure and photoplethysmography during mechanical ventilation." *Anesthesia & Analgesia*, 2006. **103**(5): p. 1182–8.

23. Crystal, G.J. and M.R. Salem, "The Bainbridge and the "reverse" Bainbridge reflexes: history, physiology, and clinical relevance." *Anesthesia & Analgesia*, 2012. **114**(3): p. 520–32.

24. Chon, K.H., S. Dash, and K. Ju, "Estimation of respiratory rate from photoplethysmogram data using time-frequency spectral estimation." *IEEE Transactions on Bio-medical Engineering*, 2009. **56**(8): p. 2054–63.

25. Tavakoli, M., L. Turicchia, and R. Sarpeshkar, "An Ultra-Low-Power Pulse Oximeter Implemented with an Energy-Efficient Transimpedance Amplifier." *IEEE Transactions on Biomedical Circuits and Systems*, 2010. **4**(1): p. 27–38.

26. Poh, M., N. Swenson, and R. Picard, "Motion-Tolerant Magnetic Earring Sensor and Wireless Earpiece for Wearable Photoplethysmography." *IEEE Transactions on Information Technology in Biomedicine*, 2010. **14**(3): p. 786–794.

REPORT DOCUMENTATION PAGE

1. REPORT DATE *(DD-MM-YYYY)*	2. REPORT TYPE	3. DATES COVERED *(From - To)*
19 Nov 2012 (Reissued 2/11/13)	Project Report	

4. TITLE AND SUBTITLE	5a. CONTRACT NUMBER
FY12 Line-Supported Bio-Medical Initiative Program: Advanced Photoplethysmography (PPG) Sensors for Operational and Casualty Care Medicine	FA8721-05-C-0002
	5b. GRANT NUMBER
	5c. PROGRAM ELEMENT NUMBER

6. AUTHOR(S)	5d. PROJECT NUMBER
Albert J. Swiston and Milan Raj	2232
	5e. TASK NUMBER
	1001
	5f. WORK UNIT NUMBER

7. PERFORMING ORGANIZATION NAME(S) AND ADDRESS(ES)	8. PERFORMING ORGANIZATION REPORT NUMBER
MIT Lincoln Laboratory 244 Wood Street Lexington, MA 02420-9108	LSP-40

9. SPONSORING / MONITORING AGENCY NAME(S) AND ADDRESS(ES)	10. SPONSOR/MONITOR'S ACRONYM(S)
ASD(R&E) 3000 Defense Pentagon Washington, DC 20302-3000	
	11. SPONSOR/MONITOR'S REPORT NUMBER(S)
	ESC-EN-HA-TR-2012-116

12. DISTRIBUTION / AVAILABILITY STATEMENT

Approved for public release; distribution is unlimited.

13. SUPPLEMENTARY NOTES

14. ABSTRACT

Visible and near-infrared light interact via absorption and scattering with biomolecules, and a number of diagnostic tools based upon these interactions have been developed to indicate pathophysiological states and normal and diseased tissue. Additionally, the cyclic nature of these absorption or scattering events, such as those arising from cardiovascular or pulmonary physiology, has recently been shown to indicate trauma and cardiovascular status. The most commonly encountered diffuse optical technique is pulse oximetry, a form of photoplethysmography (PPG), where the distinct absorption behavior of oxygenation and non-oxygenation hemoglobin molecules forms a basis for determining arterial blood O_2 saturation levels (SpO_2). New analysis algorithms have shown that PPG can be used to indicate a variety of physiological conditions beyond hypoxic hypoxemia (i.e., low SpO_2) including noncompressible hemorrhage, a condition notoriously difficult to diagnose without CT or MRI capabilities, and cardiac output, a variable difficult to measure in real time noninvasively.

With support from the FY12 Biomedical Initiative Line, we embarked on a size, weight, and power (SWaP) analysis of PPG sensors, and collaborated with Professors Ki Chon and Yitzhak Mendelson from Worcester Polytechnic Institute to build a prototype ultra-low SWaP sensor. This report gives background and motivation for why PPG sensing is an important physiological modality, and details on the SWaP analysis and prototype development.

15. SUBJECT TERMS

16. SECURITY CLASSIFICATION OF:			17. LIMITATION OF ABSTRACT	18. NUMBER OF PAGES	19a. NAME OF RESPONSIBLE PERSON
a. REPORT Unclassified	b. ABSTRACT Unclassified	c. THIS PAGE Unclassified	Same as report	38	19b. TELEPHONE NUMBER *(include area code)*